

# Determination of post-mortem interval using *in situ* tissue optical fluorescence

Éverton Sérgio Estracanholi<sup>1,\*</sup>, Cristina Kurachi<sup>1</sup>, José Renato Vicente<sup>1</sup>, Priscila Fernanda Campos de Menezes<sup>1</sup>, Orlando Castro e Silva Júnior<sup>2</sup>, Vanderlei Salvador Bagnato<sup>1</sup>

<sup>1</sup> Instituto de Física de São Carlos - Universidade de São Paulo, Av. Trabalhador São-Carlense 400, São Carlos, SP, 13566-590 Brazil

<sup>2</sup> Faculdade de Medicina de Ribeirão Preto - Universidade de São Paulo, Av. Bandeirantes 3900, Ribeirão Preto, SP, 14049-900 Brazil

\* [evertonse@ursa.ifsc.usp.br](mailto:evertonse@ursa.ifsc.usp.br)

**Abstract:** In this study we have used fluorescence spectroscopy to determine the post-mortem interval. Conventional methods in forensic medicine involve tissue or body fluids sampling and laboratory tests, which are often time demanding and may depend on expensive analysis. The presented method consists in using time-dependent variations on the fluorescence spectrum and its correlation with the time elapsed after regular metabolic activity cessation. This new approach addresses unmet needs for post-mortem interval determination in forensic medicine, by providing rapid and *in situ* measurements that shows improved time resolution relative to existing methods.

© 2009 Optical Society of America

**OCIS Codes:** (170.4580) Optical diagnostics for medicine; (170.6280) Spectroscopy, fluorescence and luminescence;

---

## References and links

1. P. Vanezis, and O. Trujillo, "Evaluation of hypostasis using a colorimeter measuring system and its application to assessment of the post-mortem interval (time of death)," *Forensic Sci. Int.* **78**(1), 19–28 (1996).
2. E. Scheurer, M. Ith, D. Dietrich, R. Kreis, J. Hüsler, R. Dirnhofer, and C. Boesch, "Statistical evaluation of time-dependent metabolite concentrations: estimation of post-mortem intervals based on *in situ* 1H-MRS of the brain," *NMR Biomed.* **18**(3), 163–172 (2005).
3. A. J. Sabucedo, and K. G. Furton, "Estimation of postmortem interval using the protein marker cardiac Troponin I," *Forensic Sci. Int.* **134**(1), 11–16 (2003).
4. L. A. Johnson, and J. A. J. Ferris, "Analysis of postmortem DNA degradation by single-cell gel electrophoresis," *Forensic Sci. Int.* **126**(1), 43–47 (2002).
5. A. D. Stan, S. Ghose, X. M. Gao, R. C. Roberts, K. Lewis-Amezcuca, K. J. Hatanpaa, and C. A. Tamminga, "Human postmortem tissue: what quality markers matter?" *Brain Res.* **1123**(1), 1–11 (2006).
6. B. Zhou, L. Zhang, G. Zhang, X. Zhang, and X. Jiang, "The determination of potassium concentration in vitreous humor by low pressure ion chromatography and its application in the estimation of *postmortem* interval," *J. Chromatogr. B Analyt. Technol. Biomed. Life Sci.* **852**(1-2), 278–281 (2007).
7. B. Madea, and A. Rödiger, "Time of death dependent criteria in vitreous humor: accuracy of estimating the time since death," *Forensic Sci. Int.* **164**(2-3), 87–92 (2006).
8. D. Querido, "A preliminary investigation into postmortem changes in skinfold impedance during the early postmortem period in rats," *Forensic Sci. Int.* **96**(2-3), 107–114 (1998).
9. M. J. Prieto-Castelló, J. P. Hernández del Rincón, C. Pérez-Sirvent, P. Alvarez-Jiménez, M. D. Pérez-Cárceles, E. Osuna, and A. Luna, "Application of biochemical and X-ray diffraction analyses to establish the postmortem interval," *Forensic Sci. Int.* **172**(2-3), 112–118 (2007).
10. T. E. Huntington, L. G. Higley, and F. P. Baxendale, "Maggot development during morgue storage and its effect on estimating the post-mortem interval," *J. Forensic Sci.* **52**(2), 453–458 (2007).
11. J. Amendt, C. P. Campobasso, E. Gaudry, C. Reiter, H. N. LeBlanc, M. J. Hall; European Association for Forensic Entomology, "Best practice in forensic entomology--standards and guidelines," *Int. J. Legal Med.* **121**(2), 90–104 (2007).
12. G. A. Wagnières, W. M. Star, and B. C. Wilson, "In vivo fluorescence spectroscopy and imaging for oncological applications," *Photochem. Photobiol.* **68**(5), 603–632 (1998).
13. V. B. Loschenov, V. I. Konov, and A. M. Prokhorov, "Photodynamic therapy and fluorescence diagnostics," *Laser Phys.* **10**, 1188–1207 (2000).
14. G. K. Stookey, "The evolution of caries detection," *Dimensions of Dental Hygiene* **10**, 12–14 (2003).

15. C. Meller, C. Heyduck, S. Tranaeus, and C. Splieth, "A new in vivo method for measuring caries activity using quantitative light-induced fluorescence," *Caries Res.* **40**(2), 90–96 (2006).
  16. A. G. Doukas, M. Bamberg, R. Gillies, R. Evans, and N. Kollias, "Spectroscopic determination of skin viability. A predictor of postmortem interval," *J. Forensic Sci.* **45**(1), 36–41 (2000).
  17. A. M. C. Davies, and T. Fearn, "Back to basics: the principles of principal component analysis," *Spectroscopy Europe* **16**(6), 20–23 (2005).
  18. L. F. Costa, *Shape analysis and classification: theory and practice.* (Crc Press, 2001).
- 

## 1. Introduction

The determination of the post-mortem interval (PMI) is one of the most significant parameters for forensic medicine, especially when considering a crime elucidation. To date, several techniques have been used to determine the PMI, but most of them require some type of biopsy or collected biological fluids and laboratory tests. Others are based on subjective evaluation, such as decrease in body temperature, formation of hypostasis and lividity, muscle relaxation, cadaveric spasm and blood coagulation. Besides the possibility of altering the crime scene, these methods are time consuming and cannot be performed *in situ*, resulting in a delayed and less efficient investigation. Traditional methods for PMI determination present a time precision of approximately 25 hours for the first 100 hours of post-mortem interval [1–11]. Therefore, the development of techniques which enable objective, quantitative and with high time resolution is of great need in forensic medicine. Fluorescence spectroscopy is an optical technique that has been showing vast use in analytical chemistry and enough sensitivity and specificity for the detection of cancer and dental caries among many other biological tissue changes [12–15]. The major advantage of optical techniques in tissue characterization is the possibility of a real time response through a non-invasive and non-destructive investigation. The aim of the present study was to evaluate the efficacy of fluorescence spectroscopy in the determination of the PMI. The hypothesis tested here was that the skin alterations occurring after the animal death result in fluorescence changes that may be detected by spectroscopic measurement and correlated to the PMI. The study by AG Doukas et al. (2000), was the first to report the use of fluorescence spectroscopy to PMI determination in skin [16], and besides this reference, we have no knowledge of any other experimental study. It is worth to be noted that in the referred study, the authors used a fluorescent marker to evaluate skin fluorescence and correlate with PMI. In our study, we based our analysis on skin autofluorescence related to temporal tissue changes.

## 2. Materials and methods

In this study 45 male *Wistar* rats were used and divided in training and validation groups with 35 and 10 animals, respectively. In the training group 7 animals were investigated for each PMI of 0, 24, 48, 72, and 96 hours. The animals were killed in a CO<sub>2</sub> gas chamber and maintained in a laboratory fume hood, with controlled filtered air, until the fluorescence measurements were done. Just before the fluorescence interrogation, the hair was manually removed providing a 2cm x 2cm skin area at the abdomen. This procedure adds some variability in fluorescence measurement, but it is the most efficient way to avoid the hair effect in this animal model.

The used fluorescence spectroscopy system was composed by a spectrometer (SF2000 – Ocean Optics, USA), 420nm and 540nm longpass filters, a desktop with a data acquisition software (OOIBase – Ocean Optics, USA), two excitation lasers, and a Y-type optical fiber probe. The excitation wavelengths at 408nm and 532nm were provided by a diode laser and the doubled-frequency of a Nd:YAG laser, respectively. Those excitation wavelengths are related as in the appropriate spectral region for light induced fluorescence of biological tissues.

The interrogation tip of the probe was perpendicularly placed in gentle contact with the skin. The y-type probe is composed by 2 optical fibers of 400 μm diameter, one for excitation and the other for light collection. For each animal and each excitation wavelength, 40 fluorescence spectra were measured. As a result, 280 fluorescence spectra for each PMI and excitation wavelength were collected.

The fluorescence spectra from the training group were processed using two distinct mathematical methods. For the spectral data obtained with 532nm excitation, the analysis was based on temporal monitoring of the intensity ratio of two emission bands ( $\lambda_1 = 600\text{nm}$  and  $\lambda_2 = 630\text{nm}$ ). For the data with 408 excitation a multivariate analysis based on Principal Component Analysis (PCA) was performed on the whole fluorescence spectrum. An algorithm was constructed for each spectrum processing method and applied for the data from the validation group, using Matlab<sup>®</sup>7 (The MathWorks, USA) platform. From the results, the obtained time resolution of PMI determination were compared to commonly reported performance achieved by the most used conventional methods.

### 3. Results

Skin autofluorescence spectra induced by excitation at 408nm and 532nm are quite distinct (Fig. 1(a) and 1(c)). Spectral variation in shape and intensity could be observed even between measurements at the same animal and the same PMI for both excitation wavelengths. Spectral differences were also noted between animals and investigation times. These variances were expected since this method is based on point spectroscopy, interrogating a small tissue volume, and local biochemical and structural variations may be reflected at the measured fluorescence spectra. Additionally, besides the variation that occurs between interrogation sites at the same PMI, tissue degradation after death is a process that does not show uniform progression within the organ. Uncertainty of these variables, together with the natural biodiversity, contributed to a diversity of spectral behavior. The pressure of the optical probe during the fluorescence measurement plays an important role when considering *in vivo* evaluation. Changes on fluorescence intensity and spectrum can be observed mainly due to distinct blood flow in the interrogated microenvironment when different pressures are applied between fiber probe and tissue. We performed a simple test in a dead animal evaluating the skin fluorescence spectral changes when different manual pressures were applied at the probe during the measurements. Even though no significant changes could be noticed, we were aware that this variance was contained in the measurement. All this inherent variance associated with the skin post-mortem process and the animal model here investigated reflects on the spectral variance observed in Fig. 1(a) and 1(c). Those spectra of Fig. 1(a) and 1(c) also exemplify variations observed in the measurements for animal within the same group and measuring sites (PMI = 24 hours).

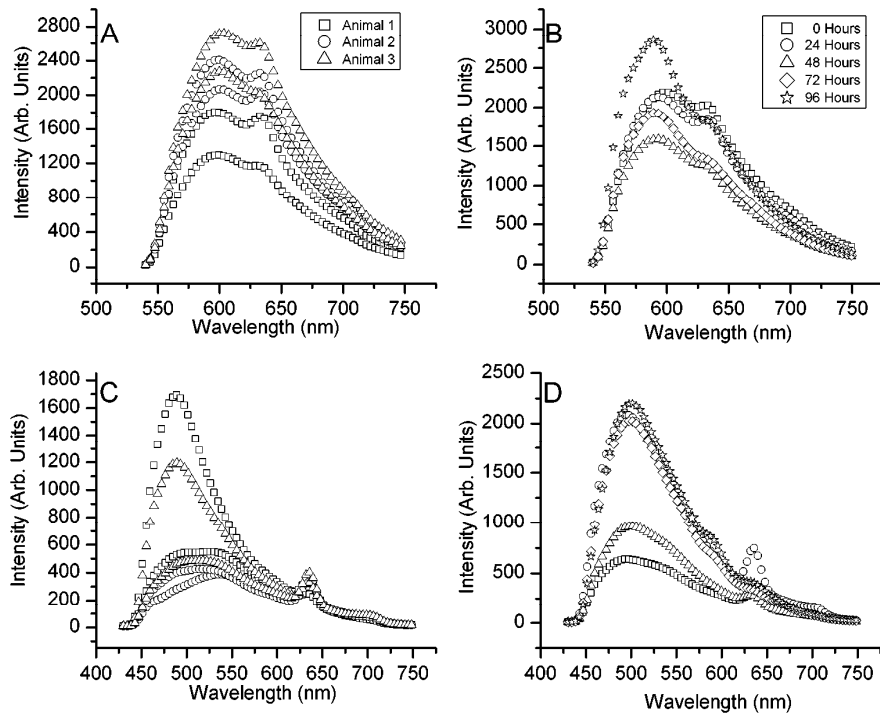


Fig. 1. Spectral variation observed at distinct interrogation sites and animals at the same PMI for excitation at 532 nm (A) and 408 nm (C). Spectral variation observed at different PMI for excitation at 532 nm (B) and 408 nm (D).

Despite the observed inter and intra-animal variance, a time dependent spectral feature could be discriminated using 532nm excitation, as shown by the presence of two typical emission bands at 600nm and 630nm, with distinct evolution. The temporal monitoring and sample distribution of the intensity ratio  $I_{600}/I_{630}$  for the investigated PMIs are presented at Fig. 2. The vertical lines correspond to the average value for the ratio  $I_{600}/I_{630}$  for each PMI. The evolution of the average value with PMI characterizes a monotonic relation.

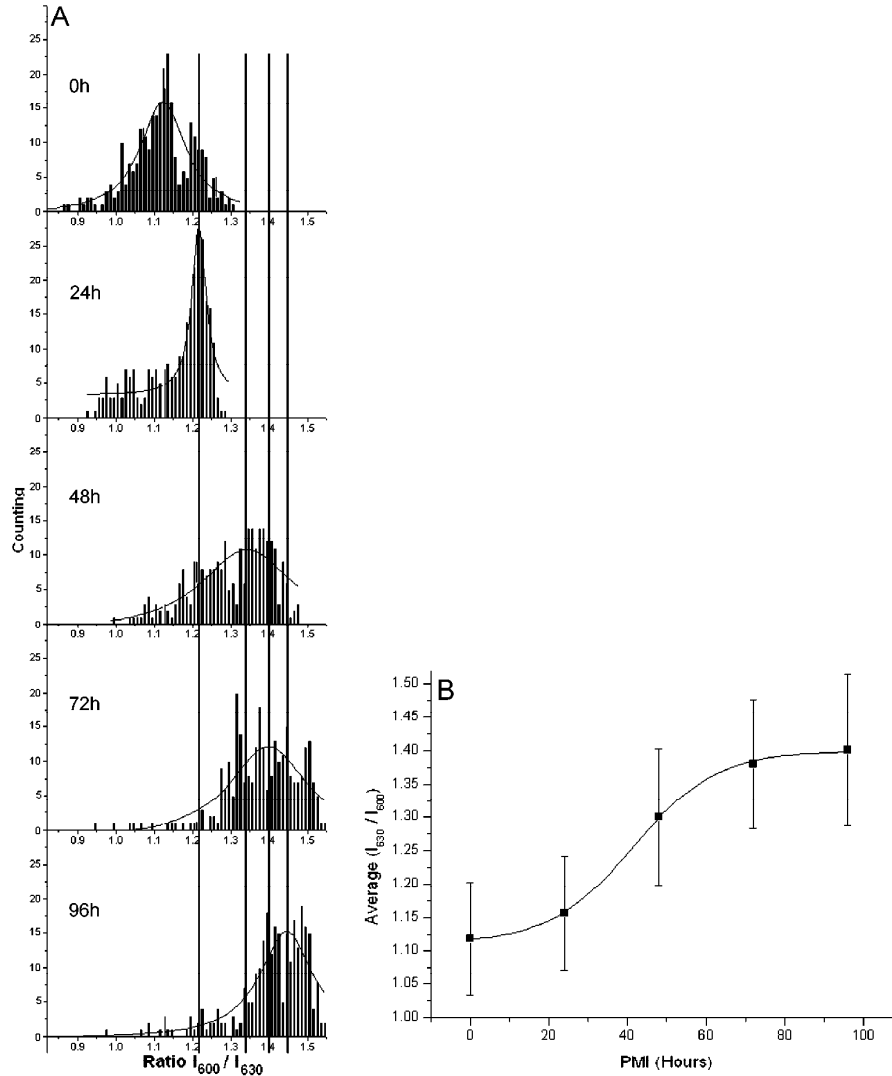


Fig. 2. (A) Evolution of the ratio intensity ( $I_{600}/I_{630}$ ) as the PMI increases. (B) Dependence of the average spectral ratio  $I_{630}/I_{600}$  with PMI.

Even though there is a large sample distribution, an increase of the average intensity ratio could be observed as a function of PMI as showed in Fig. 2(b). The error bars were taken as the standard deviation. Besides the large variation observed in the plot of Fig. 2, the final outcome of the present method can be classified as “very good”. It is relevant to note that all traditional methodologies used to extract time variation at biological tissue, result in intrinsically large dispersion in values. This is associated to many features discussed along this text. Although large dispersion is a common characteristic in this area research<sup>1-9</sup>. The possibility for a full optical procedure may introduce new advantages.

From the data of Fig. 2(b), an empirical relation between PMI and the ratio  $R = I_{630}/I_{600}$  can be obtained, which is valid for the interval of R from 1.1 to 1.4, Eq. (1).

$$R \cong 1.4 - \frac{0.3}{\left(1 + e^{\frac{PMI - 41.5}{10.6}}\right)} \quad (1)$$

For the spectral data obtained by excitation at 408nm none direct evident feature or pattern could be clearly identified. In this case, PCA was chosen as a mathematical processing method using the data from the whole measured fluorescence spectrum. This statistical method is based on a complex analysis of variance and it was used to identify the spectral properties correlated to the PMI taking into account intrinsic inter- and intra-animal variances. The PCA analysis was performed where each spectrum is a sample, each emission wavelength between 430nm and 750nm is a variable (column) and the fluorescence intensity is analyzed, representing the data matrix [17-18]. All emission wavelengths (hundreds of variables) could be reduced to two new variables: the principal components PC<sub>1</sub> and PC<sub>2</sub>. Those new variables still represent 92.4% of all information provided by the whole spectrum. Figure 3(a) shows the sample distribution in the plot PC<sub>1</sub> x PC<sub>2</sub> where each dot represents one spectrum. The sample grouping for each investigated PMI can be described by a linear behavior, showing a high correlation between PC<sub>1</sub> and PC<sub>2</sub>. For each PMI it is possible to determine the best linear function that represents the sample group (Fig. 3(a)). The angular coefficient for each line plot was determined. Figure 3(b) shows the angular coefficient obtained for all PMI with the same xy origin (set at 0,0).

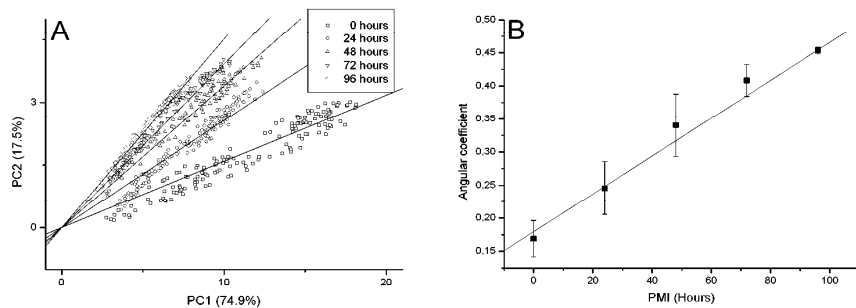


Fig. 3. (A) PC<sub>1</sub> x PC<sub>2</sub> plot showing sample distribution of all 5 investigated groups. (B) Angular coefficient determined for each PMI in PC<sub>1</sub> x PC<sub>2</sub>.

The error bars corresponds to the standard deviation and a decrease of this value can be observed after 72 hours showing that the inter-animal variances investigated at 408nm induced fluorescence also decrease at that time interval.

Considering the first degree relation between the angular coefficient and time interval, a second algorithm for PMI determination is determined by Eq. (2).

$$A = \frac{PMI + 58}{328} \quad (2)$$

where A is the angular coefficient obtained in PC<sub>1</sub> x PC<sub>2</sub> plot.

Using the algorithms determined by the two alternative ways in which spectral data was processed, the PMI of 10 animals (validation group) was determined, as seen in Fig. 4. Figures 4(a) and 4(b) represent the correlation of the determined and real PMIs for intensity ratio analysis and PCA, respectively. If the values of determined and real PMI were equivalent, all the points of the PMI<sub>Real</sub> x PMI<sub>Determined</sub> plot would be within the dashed line. Even though these values were not coincident, a high correlation is obtained (solid line) when compared to an ideal estimation (dashed line). Although, the obtained deviation can be

corrected if extra terms were added to Eq. (1), this was not performed in this study. For both spectra analyses performed, a high correlation coefficient was obtained, 0.99 for the intensity ratio analysis and 0.96 for PCA. Correlation coefficient<sup>8</sup> is a measure of how well the predicted values from a forecast model fit with the real data. High correlation is necessary but is not enough to evaluate the efficiency of the employed method.

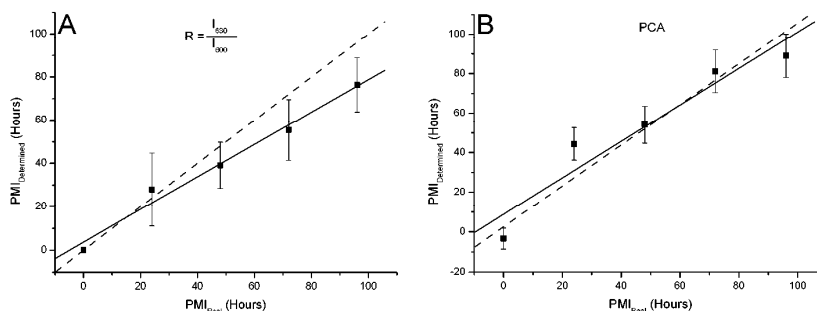


Fig. 4. Correlation plots of real and estimated PMI determined by intensity ratio  $I_{630}/I_{600}$  (A) and by PCA (B).

The ideal correlation between the real and determined PMI corresponds to the dashed line in Fig. 4 (both methods), which would imply an angular coefficient between  $PMI_{Real}$  and  $PMI_{Determined}$  of value 1. Our proposed methods of intensity ratio analysis and PCA achieved angular coefficients of 0.75 and 0.92, respectively. In this sense, the PCA showed a higher efficiency in the PMI prediction. We are confident, especially when considering the precision of the conventional methods, that the correlation between predicted and real is a significant improvement, especially when considering all variations pertinent to a biological sample.

One can compare the precision here obtained with other methods<sup>1-9</sup> applied within the zero to hundred hours PMI determination. In Table 1 we present the precision in hours for conventional methods based on the standard deviation considered the reported experimental data. The presented precision of 20 hours is already acceptable relative to traditional methodology. Furthermore, our approach offers the possibility for further improvements, such as by the capability of integrating multi-excitation analyses and time resolved fluorescence.

**Table 1. Present chronotatognosis techniques: animal studies where the PMI was predicted and the standard deviation calculated. Results were obtained from our interpretation of the published data.**

Method	Animal Model	PMI Analyzed (h)	Standard Deviation (h)
Hypostasis colour <sup>1</sup>	Human	0 - 30	16
		0 - 72	24
Concentration of H-MRS in the brain <sup>2</sup>	Sheep	50 - 100	10
		100 - 200	50
Protein degradation (Troponin I) <sup>3</sup>	Bovine	0 - 10	9
		0 - 70	20
DNA Degradation <sup>4</sup>	Human	3 - 56	15
RNA Integrity <sup>5</sup>	Human	0 - 40	10
Concentration of K <sup>+</sup> in vitreous humor <sup>6</sup>	Human	0 - 30	10

<b>Concentration of K<sup>+</sup> in vitreous humor<sup>7</sup></b>	Human	0 - 133	23
<b>Skin Impedance variation<sup>8</sup></b>	Rats	0 - 120	27
H-MRS:Proton Magnetic Resonance Spectroscopy; DNA:Deoxyribonucleic Acid; RNA:Ribonucleic Acid.			

#### 4. Conclusion

The presented results and methodology demonstrated the use of fluorescence tissue spectroscopy for the determination of PMI as a valuable tool in forensic medicine.

Two approaches were employed to associate the spectral changes with the time evolution of tissue modification. First, direct spectral changes were computed through inter-spectra analysis, allowing the establishment of a pattern of the sample distribution with time evolution. Second, using a statistical method based on PCA well identified features with time progression were produced. In both cases, the characteristic pattern time evolution presented a high correlation coefficient, indicating that the chosen pattern presented direct linear relationship with time. The close to unit angular coefficients obtained during comparison between  $PMI_{Real}$  and  $PMI_{Determined}$  demonstrated that both methods can be used as determination of PMI. However, when comparing the two proposed methods, PCA showed to be superior.

Besides being a new method, with compatible precision or even higher than existent methods, the results can be readily improved if new concepts as multi-wavelength excitation and others are used, providing more variables and new possibilities. Such realizations will constitute the basis for new studies.

#### Acknowledgements

Financial support from FAPESP, CAPES and CNPq, Brazilian funding agencies. Special thanks are extended to Dr. Marco Aurélio Guimarães (Medical School of Ribeirão Preto) for comments and suggestions and to Dr. Glauco Ranna Souza for critical reading.